Lattice Boltzmann simulations of decaying homogeneous isotropic turbulence

Huidan Yu,[1,*] Sharath S. Girimaji,[1,†] and Li-Shi Luo[2,‡]

[1]*Department of Aerospace Engineering, Texas A & M University, College Station, Texas 77843-3141, USA*
[2]*Department of Mathematics & Statistics, Old Dominion University, Norfolk, Virginia 23529, USA*

Decaying homogeneous isotropic turbulence in inertial and rotating reference frames is investigated to evaluate the capability of the lattice Boltzmann method in turbulence. In the inertial frame case, the decay exponents of kinetic energy and dissipation and the low wave-number scaling of the spectrum are studied. The results are in agreement with classical ones. In the frame-rotation case, simulations show that the energy decay rate decreases with decreasing Rossby number as the energy cascade is inhibited by rotation, again in agreement with turbulence physics. These results clearly indicate that the lattice Boltzmann method captures important features of decaying turbulence.

　　　　PACS number(s): 47.11.+j, 47.27.−i, 34.50.Ez, 47.32.−y

The lattice Boltzmann equation (LBE) [1–6] is rapidly becoming a viable alternative for computing fluid flows. The lattice Boltzmann method (LBM) is based on the Boltzmann equation and kinetic theory rather than the Navier-Stokes (NS) equations and continuum theory [7]. The Boltzmann equation constitutes the core of mesoscopic theory which relates the macroscopic equations for flow systems to the underlying microscopic molecular dynamics. The methods based on the Boltzmann equation, such as the LBE method, are more general than the ones based on the NS equations because kinetic methods may be applied to extended hydrodynamics for which continuum theory is invalid. In addition to theoretical generality, kinetic methods may have computational and numerical advantages because the Boltzmann equation is a first-order linear partial different equation (PDE) as opposed to the NS equation, a second order nonlinear PDE. It has been argued that discretization of first-order linear PDEs has the following advantages [8]. First, first-order linear PDEs require only the smallest possible stencil for accurate discretization, may be easier to achieve convergence, and yield the highest potential discretization accuracy on nonsmooth, adaptively refined grids. Second, stiff terms in first-order PDEs are local in nature thus can be handled by local solution techniques, as opposed to global ones. And third, systems of first-order PDEs are better suited for functional decomposition than the traditional higher-order nonlinear PDEs [8]. Consequently, LBM has found applications in many areas of flow physics (cf. reviews [9–12] and references therein).

In this paper, we focus on the application of LBE to turbulence. As a first step to evaluate the capability of LBE in turbulence, we conduct direct numerical simulations (DNS) of decaying homogeneous isotropic turbulence (DHIT) in both inertial and rotating frames of reference. DHIT is an important benchmark problem in the field of DNS of turbulence. The first attempt at DNS of NS equation in fact involved DHIT [13]. Recent investigations include studies on decay exponents and low wave-number spectra using NS-DNS [14–16]. Some preliminary three-dimensional (3D) DHIT studies using LBE have also been performed [17–19] but they stop well short of quantitative comparisons with classical results. The objective of this work is to compute DHIT with LBE and perform detailed comparisons with established results on the following important issues: (i) energy decay exponent, (ii) low wave-number scaling of the spectra, and (iii) effect of rotation on energy decay.

The energy spectrum $\hat{E}(\boldsymbol{\kappa},t)$ in DHIT evolves as

$$\partial_t \hat{E}(\boldsymbol{\kappa},t) = -\hat{T}(\boldsymbol{\kappa},t) - 2\nu\kappa^2 \hat{E}(\boldsymbol{\kappa},t), \qquad (1)$$

where $\boldsymbol{\kappa}$ is the wave number and ν is the viscosity, and $\hat{T}(\boldsymbol{\kappa},t)$ represents the nonlinear energy transfer between modes [cf. Eq. (6.162) in Ref. [20]]. The kinetic energy k and dissipation ϵ of turbulence are given, respectively, by

$$k = \int \hat{E}(\boldsymbol{\kappa})d\boldsymbol{\kappa} \quad \text{and} \quad \epsilon = 2\nu \int \kappa^2 \hat{E}(\boldsymbol{\kappa})d\boldsymbol{\kappa}.$$

It has been long observed that, after a short initial transient period of time, the kinetic energy k and dissipation ϵ exhibit power-law decay,

$$k(t)/k_0 \sim (t/t_0)^{-n}, \quad \epsilon(t)/\epsilon_0 \sim (t/t_0)^{-(n+1)}, \qquad (2)$$

where k and ϵ have the values k_0 and ϵ_0, respectively, at the reference time $t_0 = nk_0/\epsilon_0$. Isotropic turbulence is characterized by the Taylor-microscale Reynolds number,

$$\text{Re}_\lambda = \frac{u_{\text{rms}}\lambda}{\nu} = \sqrt{\frac{20}{3\nu\epsilon}k}, \qquad (3)$$

where $u_{\text{rms}} = \sqrt{2k/3}$ is the root mean square (rms) of the velocity field $\boldsymbol{u}$ and $\lambda = \sqrt{15\nu u_{\text{rms}}^2/\epsilon}$ is the transverse Taylor-microscale length.

Equation (1) admits a continuous class of invariant solutions in the limit of Re→∞. At the large Re, $\hat{E}(\boldsymbol{\kappa},t)$ at the low wave number behaves as $\lim_{\kappa\to 0} \hat{E}(\kappa) \sim \kappa^\sigma$, where σ is a

──────────
*Electronic address: h0y5840@aero.tamu.edu
†Electronic address: girimaji@aero.tamu.edu
‡Electronic address: lluo@odu.edu; URL: http://www.lions.odu.edu/˜lluo

time-independent constant (e.g. Ref. [21]). For inviscid fluids, if Loitsyansky's integral [22] is an invariant, then $\sigma=4$ and $n=10/7$ [23]; if Birkhoff's integral [24] is an invariant, then $\sigma=2$ and $n=6/5$ [25]. It has been recently shown that constant integral length scale l or the Reynolds number Re correspond to $\sigma=\infty$ and $n=2$ or $\sigma=1$ and $n=1$, respectively [26]. Furthermore, the conservations of energy, angular momentum, and helicity lead to $\sigma=2$, 7, and 1, in the limit of Re$\rightarrow\infty$, respectively. The energy conservation of inviscid fluids uniquely determines the invariant solution of Eq. (1), i.e., $\sigma=2$, in accordance with Birkhoff's invariant [24]. Despite the apparent simplicity of the DHIT problem, the relevant flow invariant, asymptotic decay exponent, and the low-κ scaling are strong functions of the initial spectrum and Reynolds number. There is still no clear consensus on whether the angular momentum or energy is the correct invariant. It is also not clear what the conditions are under which the invariance of either quantity can be observed. As a result, several different outcomes have been reported in the literature [14,15,27,28].

The lattice Boltzmann equation with single-relaxation-time approximation due to Bhatnagar, Gross, and Krook (BGK) [29] for the collision operator is [2,3]

$$f_\alpha(\boldsymbol{x}+\boldsymbol{e}_\alpha\delta_t,t+\delta_t)=f_\alpha(\boldsymbol{x},t)-\frac{1}{\tau}[f_\alpha-f_\alpha^{(eq)}]+F_\alpha, \quad (4)$$

where f_α is the density distribution function with the discrete velocity $\boldsymbol{e}_\alpha$, $f_\alpha^{(eq)}$ is the equilibrium distribution function, and τ is the relaxation time determining the viscosity ν of the modeled fluid. We use the 3D 19-velocity model (D3Q19) in our simulations because of its robust numerical characteristics [30]. The equilibria for incompressible flow [31] are

$$f_\alpha^{(eq)}=w_\alpha\left\{\delta\rho+\rho_0\left[\frac{3\boldsymbol{e}_\alpha\cdot\boldsymbol{u}}{c^2}+\frac{9(\boldsymbol{e}_\alpha\cdot\boldsymbol{u})^2}{2c^4}-\frac{3u^2}{2c^2}\right]\right\},$$

where $\delta\rho$ is the density fluctuation, and ρ_0 is the mean density in the system which is usually set to 1, and $c=\delta_x/\delta_t=1$ in lattice units. The sound speed of the model is $c_s=c/\sqrt{3}$. The total density is $\rho=\rho_0+\delta\rho$. The discrete particle velocities $\boldsymbol{e}_\alpha$ are

$$\boldsymbol{e}_\alpha=\begin{cases}(0,0), & \alpha=0\\(\pm1,0,0),(0,\pm1,0),(0,0,\pm1), & \alpha=1\text{--}6\\(\pm1,\pm1,0),(\pm1,0,\pm1),(\pm1,\pm1,0), & \alpha=7\text{--}18,\end{cases}$$

and the weighting coefficients are: $w_0=1/3$, $w_{1-6}=1/18$, $w_{7-18}=1/36$. The mass and momentum conservations are enforced:

$$\delta\rho=\sum_\alpha f_\alpha=\sum_\alpha f_\alpha^{(eq)},$$

$$\rho_0\boldsymbol{u}=\sum_\alpha \boldsymbol{e}_\alpha f_\alpha=\sum_\alpha \boldsymbol{e}_\alpha f_\alpha^{(eq)}.$$

For isothermal fluids, the forcing term F_α is [32]

$$F_\alpha=-3w_\alpha\rho_0\frac{\boldsymbol{e}_\alpha\cdot\boldsymbol{a}}{c^2}\delta_t, \quad (5)$$

where $\boldsymbol{a}$ is the acceleration due to external force. Here, we consider the Coriolis force, i.e., $\boldsymbol{a}=-2\boldsymbol{\Omega}\times\boldsymbol{u}$, where $\boldsymbol{\Omega}$ is the angular velocity of the frame of reference.

The hydrodynamic equations derived from Eq. (4) through the Chapman-Enskog analysis are

$$\partial_t\rho+\boldsymbol{\nabla}\cdot\rho\boldsymbol{u}=0, \quad (6a)$$

$$\partial_t\boldsymbol{u}+\boldsymbol{u}\cdot\boldsymbol{\nabla}\boldsymbol{u}=-\boldsymbol{\nabla}p+\nu\nabla^2\boldsymbol{u}+\boldsymbol{a}, \quad (6b)$$

where $p=c_s^2\rho/\rho_0$ and the viscosity $\nu=c_s^2(\tau-1/2)$.

The strain tensor S can be obtained directly from the non-equilibrium part of the distribution functions

$$\mathsf{S}=-\frac{1}{2\rho_0 c_s^2\tau}\sum_\alpha \boldsymbol{e}_\alpha\boldsymbol{e}_\alpha[f_\alpha-f_\alpha^{(eq)}], \quad (7)$$

and $\epsilon=2\nu\langle\mathsf{S}:\mathsf{S}\rangle$, where $\langle\rangle$ denotes volume averaging.

The initial incompressible homogeneous isotropic velocity field $\boldsymbol{u}_0$ ($\boldsymbol{\nabla}\cdot\boldsymbol{u}_0=0$) is generated in $\boldsymbol{\kappa}$ space with the following energy spectrum with random phase:

$$\hat{E}(\boldsymbol{\kappa},0)=\begin{cases}0.038\kappa^m e^{-0.14\kappa^2}, & \kappa\in[\kappa_{\min},\kappa_{\max}],\\0, & \kappa\notin[\kappa_{\min},\kappa_{\max}].\end{cases} \quad (8)$$

We use different values of m in Eq. (8) to test the effect due to the initial spectrum. We use $m=4$ in what follows unless otherwise stated.

A successful LBE turbulence simulation hinges upon precise stipulation of initial conditions. For Navier-Stokes based turbulence simulations, one only needs to specify an initial velocity field. For decaying isotropic turbulence simulations, a random, isotropic, and divergence-free velocity field $\hat{\boldsymbol{u}}_0$ of a required spectrum $\hat{E}(\boldsymbol{\kappa},0)$ in spectral space $\boldsymbol{\kappa}$ is generated, following the, now standard, procedure described in Refs. [33,34]. The initial pressure is then obtained by solving the Poisson equation. However, the initialization in the LBE simulations has to be done differently because, first of all, unlike incompressible Navier-Stokes simulations, the LBE method is inherently compressible. Moreover, all the distribution functions $\{f_\alpha\}$, not just their conserved moments ρ (or p) and $\rho\boldsymbol{u}$, must be initialized in a self-consistent manner. This can be best understood in terms of the generalized or multiple-relaxation-time (MRT) LBE [4–6]. Given an LBE model with Q discrete velocities in D dimensions, the Q distribution functions $\{f_\alpha\}$ are equivalent to Q moments $\{m_\alpha\}$. The velocity and pressure fields only specify $(D+1)$ conserved moments of $\{f_\alpha\}$, and usually $(D+1)\ll Q$. To obtain accurate results for HIT simulations by using LBE, it is imperative to properly initialize all of the $\{f_\alpha\}$, or equivalently the moments $\{m_\alpha\}$. Clearly it is difficult, if at all possible, to accurately and consistently estimate the nonconserved moments, which are related to the derivatives of the conserved moments ρ and $\boldsymbol{u}$, for a given $\boldsymbol{u}_0$. Thus an effective initialization procedure is needed [35].

We now describe the iterative procedure proposed in Ref. [35] within the context of the lattice BGK (LBGK) equation.
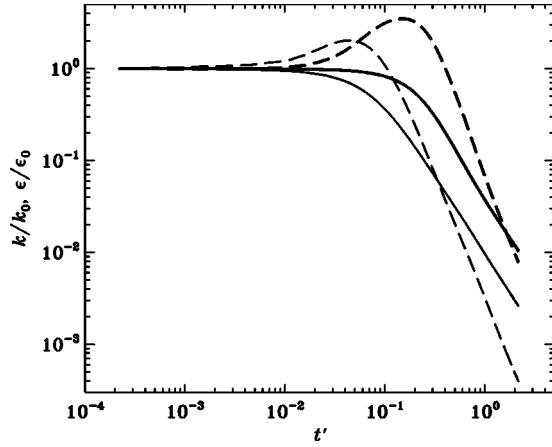
FIG. 1. Time evolution of the normalized kinetic energy k/k_0 (solid lines) and normalized dissipation rate ϵ/ϵ_0 (dashed lines) for 64^3 (thin lines) and 128^3 (thick lines) cube.

First, we generate a random, isotropic, and divergence-free velocity field u_0 of the required spectrum $\hat{E}(\kappa,0)$ in the spectral space κ using the procedure outlined in Ref. [33,34]. The initial velocity is then transferred back to the real space x. Then the LBGK equation (4) without external force F_α is used iteratively to compute the distribution functions $\{f_\alpha\}$ (and $\delta\rho$) with the velocity field u fixed at the initial velocity field u_0, that is, in the LBGK collision process, the equilibria are given by

$$f_\alpha^{(eq)} = f_\alpha^{(eq)}(\delta\rho, u_0),$$

where $\delta\rho$ is updated at each time step while the velocity field is fixed at the given initial field u_0. This iteration with a fixed initial velocity field u_0 leads to the values of $\{f_\alpha\}$ consistent with u_0. It can be shown that the pressure p so obtained is indeed the correct solution of the Poisson equation [36].

We observe that, without proper initialization of $\{f_\alpha\}$, the initial equilibration process can generate strong acoustic (pressure) waves through the system which can persist for long time. Two severe consequences may result from the unphysical initial acoustic disturbances. First, the acoustic disturbances may lead to numerical instability and this is particularly severe in the LBGK models, because the LBGK models do not have an adequate amount of the bulk viscosity to dissipate the acoustic disturbances. The second undesirable consequence of inconsistent initialization is that initial acoustic disturbances can significantly contaminate the solution at later times. For instance, the total energy can be a few percent less than its correct value if the initialization is incorrect. The proposed initialization procedure [35] significantly reduces the magnitude of initial acoustic disturbances, and it has also been successfully applied to LBE-LES simulations [37].

We first simulate DHIT in the inertial frame. We use two system sizes: 64^3 and 128^3. The initial energy spectrum is nonzero in the range $[\kappa_{min}, \kappa_{max}]=[4,8]$ and $[1,8]$, according to Eq. (8), for 64^3 and 128^3, respectively; and $u_{rms}=0.023$ and $\nu=1/600$ ($\tau=0.505$), resulting in $Re_\lambda \approx 53$ for 64^3 and 270 for 128^3.
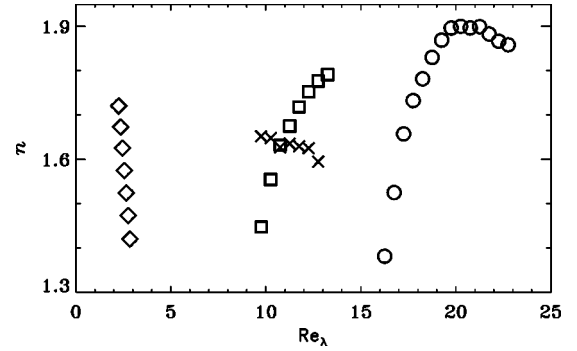

FIG. 2. The decay exponent n depending on initial conditions and Re_λ. For the 128^3 cube, ◇: $u_{rms}=0.0064$, $\nu=0.01$, and $[\kappa_{min}, \kappa_{max}]=[1,8]$; □: $u_{rms}=0.021$, $\nu=1/600$, and $[\kappa_{min}, \kappa_{max}]=[8,16]$; ○: $u_{rms}=0.022$, $\nu=1/600$, and $[\kappa_{min}, \kappa_{max}]=[1,8]$. For the 64^3 cube (×): $u_{rms}=0.022$, $\nu=1/600$, and $[\kappa_{min}, \kappa_{max}]=[4,8]$.

Figure 1 shows the evolutions of the kinetic energy k/k_0 and the dissipation ϵ/ϵ_0 with the normalized time $t'=t\epsilon_0/k_0$. In the absence of production, kinetic energy decays monotonically with time. However, as shown in Fig. 1, at early times dissipation actually increases. This increase is consistent with known turbulence physics (explained further below) and similar increase is also seen in NS-DNS results. Following this period of increased dissipation, the spectrum starts decaying at all wave numbers. The decay exponent n of the kinetic energy k in these low Re_λ simulations varies with time. Furthermore, Re_λ itself is a function of time as the turbulence decays. In Fig. 2, the variation of n vs Re_λ in various simulations are shown. The computed values of n and the dependence on Re_λ are very similar to that observed in NS-DNS works (e.g. Ref. [14]). Table I compiles the values for the decay exponent n of kinetic energy obtained in recent experimental work [27,28], NS-DNS data [14,15], and the present LBE-DNS results. The LBE-DNS values of n computed here are well within the range obtained else where, as shown in Table I.

The compensated energy spectra, $\hat{E}(\kappa,t')/\kappa^4$, of the 128^3 simulation are shown in Fig. 3. Initially, the spectrum with $m=4$ in Eq. (8) (dashed line) is narrow and soon the energy spreads to higher wave numbers (smaller scales) due to the nonlinear cascade process. This phenomenon leads to the increase of the dissipation rate in physical space, as shown in Fig. 1. This fact, in itself, is quite significant since advection

TABLE I. Recent results for the exponent n. The LBE-DNS results correspond to Fig. 2 in the present work.

$\lim_{\kappa\to 0}\hat{E}(\kappa,0)$	Re_λ	exponent n	Ref.
$\hat{E}(\kappa) \sim \kappa^2$	0–30	1.1–1.52	NS-DNS [14]
$\hat{E}(\kappa) \sim \kappa^2$	10–50	1.0–3.0	NS-DNS [15]
	28.37–43.85	1.285–1.309	expt. [27]
	4.4–5.4	1.3–1.8	expt. [28]
$\hat{E}(\kappa) \sim \kappa^4$	2.3–22.5	1.38–1.85	LBE-DNS

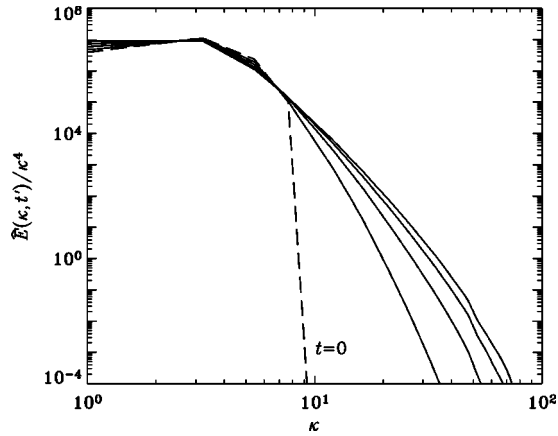FIG. 3. The compensated energy spectrum for an 128^3 simulation with $u_{rms}=0.023$ and $Re_\lambda \approx 141$, at early times, $t'=0.022$, 0.044, 0.066, and 0.088. The dashed line represents the initial spectrum of Eq. (8). The spectrum spreads to higher κ monotonically as t' increases. The spectrum scales as $\hat{E}(\kappa,t') \sim \kappa^4$ at small κ.

(the source of nonlinearity) is handled very differently in LBE. At this stage, the spectrum scales as $\hat{E}(\kappa,t') \sim \kappa^4$ at small κ. This dependence of low wave-number scaling (κ^4) on initial spectrum ($m=4$) is in agreement with the other results [14,15]. Subsequently, the spectrum starts to decay, more rapidly at the large κ and slowly at the small κ. Investigations of low wave-number scaling for other initial spectra will be performed elsewhere [37].

We also simulate DHIT in a rotating frame. Without loss of generality, we assume that the frame of reference rotates about the z axis, i.e., the angular velocity of the rotating frame of reference is $\mathbf{\Omega}=(0,0,\Omega)$. The Rossby number is defined as $Ro=\kappa_p u_{rms}/\Omega$, where κ_p characterizes the energy containing wave number at $t=0$. Here, we use $\kappa_p=(\kappa_{max}-\kappa_{min})/2$.

The effects of rotation are both scale dependent and anisotropic and they are enhanced by increasing the rotation rate Ω. In general, it has long been known [38] that rotation slows down the cascade and delays the approach to equipartition. These features are captured in Fig. 4 which shows the evolution of kinetic energy at various Rossby numbers in an 128^3 simulation. The initial energy spectrum is nonzero in the range of $1 \le \kappa \le 8$. Time is normalized by k_0/ϵ_0 of the inertial case. As expected, the energy decay slows
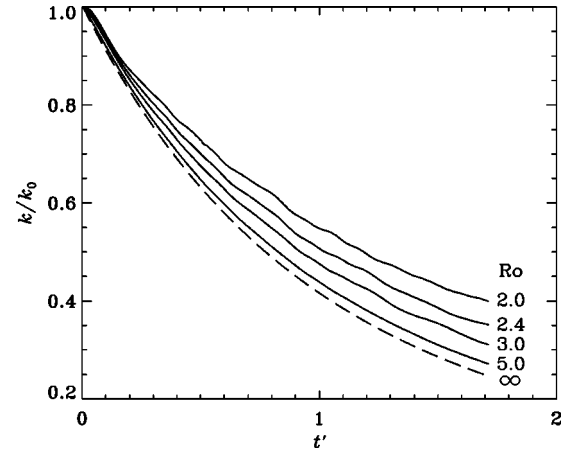

FIG. 4. Kinetic energy decay with the system size of 128^3 and different Rossby number Ro. The dashed line is the inertial case ($\mathbf{\Omega}=\mathbf{0}$ or Ro$=\infty$).

down with decreasing Rossby number (or increasing rate of rotation). Closer examination of the spectra shows the tendency to maintain more energy at the small wave numbers (large scales) when the system rotates. The faster the system rotates (smaller Rossby number), the more prominent is this tendency.

In this paper, we simulate the classical DHIT problem with LBM and reproduce well known power-law decay of the kinetic energy. The decay exponents obtained in the LBE simulations are in good agreement with experimental measurements and NS-DNS results. Correct low wave-number spectral scaling is also obtained. The effect of rotation on turbulence is to suppress the spectral cascade and thus slow down the decay.

We observe that, even though the LBE method is only second-order accurate in space and first-order in time [39–42], it compares very well with the pseudospectral method down to the scales of several grid spacings, for a reasonably long time [19]. This work further establishes the LBE method as a highly reliable DNS tool to simulate turbulence.

[1] G. R. McNamara and G. Zanetti, Phys. Rev. Lett. **61**, 2332 (1988).

[2] H. Chen, S. Chen, and H. W. Matthaeus, Phys. Rev. A **45**, R5339 (1992).

[3] Y. Qian, D. d'Humières, and P. Lallemand, Europhys. Lett. **17**, 479 (1992).

[4] D. d'Humières, in *Rarefied Gas Dynamics: Theory and Simulations*, Progress in Astronautics and Aeronautics No. 159, edited by B. D. Shizgal and D. P. Weaver (AIAA, Washington, DC, 1992), pp. 450–458.

[5] P. Lallemand and L.-S. Luo, Phys. Rev. E **61**, 6546 (2000).

[6] D. d'Humières, I. Ginzburg, M. Krafczyk, P. Lallemand, and L.-S. Luo, Philos. Trans. R. Soc. London, Ser. A **360**, 437 (2002).

[7] X. He and L.-S. Luo, Phys. Rev. E **55**, R6333 (1997); **56**, 6811 (1997).

[8] B. van Leer, Computational Fluid Dynamics: Science or Toolbox?, AIAA Report No. 2001-2520 (2001).

[9] R. Benzi, S. Succi, and M. Vergassola, Phys. Rep. **222**, 145 (1992).

[10] S. Chen and G. D. Doolen, Annu. Rev. Fluid Mech. **30**, 329 (1998).

[11] L.-S. Luo, *The Lattice-Gas and Lattice Boltzmann Methods: Past, Present and Future*, in Proceedings of the International Conference on Applied Computational Fluid Dynamics, Beijing, 2000, edited by J.-H. Wu and Z.-J. Zhu (Beijing, China, 2000), p. 52. Available at http://www.lions.odu.edu/~lluo/.

[12] D. Yu, R. Mei, L.-S. Luo, and W. Shyy, Prog. Aerosp. Sci. **39** (5), 329 (2003).

[13] S. A. Orszag and G. S. Patterson, Phys. Rev. Lett. **28**, 76 (1972).

[14] N. N. Mansour and A. A. Wray, Phys. Fluids **6**, 808 (1994).

[15] M.-J. Huang and A. Leonard, Phys. Fluids **6**, 3765 (1994).

[16] R. Samtaney, D. I. Pullin, and B. Kosović, Phys. Fluids **13**, 1415 (2001).

[17] S. Chen, Z. Wang, X. Shan, and G. D. Doolen, J. Stat. Phys. **68**, 397 (1992).

[18] R. Benzi, M. V. Struglia, and R. Tripiccione, Phys. Rev. E **53**, R5565 (1996).

[19] L.-S. Luo, L.-P. Wang, and D. Qi, in *High Performance Scientific and Engineering Computing*, edited by M. Breuer, F. Durst and C. Zenger, Lecture Notes in Computer Science Engineering No. 21 (Springer, Berlin, 2002), p. 123.

[20] S. B. Pope, *Turbulent Flows* (Cambridge University Press, Cambridge, England, 2000).

[21] J. C. Rotta, *Turbulente Strömungen* (Teubner, Stuttgart, 1972).

[22] L. G. Loitsyansky, Moscow Centr. Aero. Hydrodyn. Inst. Report No. 440, 1939 (NACA Tech. Memo, 1079).

[23] A. N. Kolmogorov, Dokl. Akad. Nauk SSSR **31**, 299 (1941).

[24] G. Birkhoff, Pure Appl. Math. **7**, 19 (1954).

[25] P. G. Saffman, J. Fluid Mech. **27**, 581 (1967).

[26] M. Oberlack, Proc. Appl. Math. Mech. **1**, 294 (2002).

[27] M. S. Mohamed and J. C. LaRue, J. Fluid Mech. **219**, 195 (1990).

[28] M. R. Smith, R. J. Donnelly, N. Goldenfeld, and W. F. Vinen, Phys. Rev. Lett. **71**, 2583 (1993).

[29] P. L. Bhatnagar, E. P. Gross, and M. Krook, Phys. Rev. **94**, 511 (1954).

[30] R. Mei, W. Shyy, D. Yu, and L.-S. Luo, J. Comput. Phys. **161**, 680 (2000).

[31] X. He and L.-S. Luo, J. Stat. Phys. **88**, 927 (1997).

[32] L.-S. Luo, Phys. Rev. E **62**, 4982 (2000).

[33] V. Eswaran and S. B. Pope, Phys. Fluids **31**, 506 (1988).

[34] P. K. Yeung and S. B. Pope, J. Fluid Mech. **207**, 531 (1989).

[35] R. Mei, L.-S. Luo, and D. d'Humières (unpublished).

[36] A. Caiazzo (unpublished).

[37] H. Yu, S. S. Girimaji, and L.-S. Luo (unpublished).

[38] Y. Yamazaki, Y. Kaneda, and R. Rubinsten, J. Phys. Soc. Jpn. **71**, 81 (2002).

[39] M. Junk and A. Klar, SIAM J. Sci. Comput. (USA) **22**, 1 (2000).

[40] M. Junk, Numer. Methods Partial Differ. Equ. **17**, 383 (2001).

[41] M. Junk and W.-A. Yong, Asymptotic Anal. **35**, 165 (2003).

[42] M. Junk, A. Klar, and L.-S. Luo (unpublished).